EBioMedicine 49 (2019) 291–304

Contents lists available at ScienceDirect

EBioMedicine

journal homepage: www.elsevier.com/locate/ebiom

Research paper

Macrophage metabolic reprogramming aggravates aortic dissection through the HIF1α-ADAM17 pathway☆ ☆

Guan Lian[a,#], Xiaopeng Li[a,#], Linqi Zhang[a], Yangming Zhang[a], Lulu Sun[a], Xiujuan Zhang[a], Huiying Liu[a], Yanli Pang[b], Wei Kong[a], Tao Zhang[c,*], Xian Wang[a,*], Changtao Jiang[a,*]

[a] Department of Physiology and Pathophysiology, School of Basic Medical Sciences, Peking University, Key Laboratory of Molecular Cardiovascular Science, Ministry of Education, Beijing 100191, China
[b] Center for Reproductive Medicine, Department of Obstetrics and Gynecology, Peking University Third Hospital, Beijing 100191, China
[c] Department of Vascular Surgery, Peking University People's Hospital, Beijing 100044, China

ARTICLE INFO

Article history:
Received 22 March 2019
Revised 23 September 2019
Accepted 25 September 2019
Available online 19 October 2019

Keywords:
HIF-1α
Macrophage
ADAM17
Aortic dissection

ABSTRACT

Background: Aortic dissection is a severe inflammatory vascular disease with high mortality and limited therapeutic options. The hallmarks of aortic dissection comprise aortic inflammatory cell infiltration and elastic fiber disruption, highlighting the involvement of macrophage. Here a role for macrophage hypoxia-inducible factor 1-alpha (HIF-1α) in aortic dissection was uncovered.

Methods: Immunochemistry, immunofluorescence, western blot and qPCR were performed to test the change of macrophage HIF-1α in two kinds of aortic dissection models and human tissues. Metabolomics and Seahorse extracellular flux analysis were used to detect the metabolic state of macrophages involved in the development of aortic dissection. Chromatin Immunoprecipitation (ChIP), enzyme-linked immunosorbent assay (ELISA) and cytometric bead array (CBA) were employed for mechanistic studies.

Findings: Macrophages involved underwent distinct metabolic reprogramming, especially fumarate accumulation, thus inducing HIF-1α activation in the development of aortic dissection in human and mouse models. Mechanistic studies revealed that macrophage HIF-1α activation triggered vascular inflammation, extracellular matrix degradation and elastic plate breakage through increased a disintegrin and metallopeptidase domain 17 (ADAM17), identified as a novel target gene of HIF-1α. A HIF-1α specific inhibitor acriflavine elicited protective effects on aortic dissection dependent on macrophage HIF-1α.

Interpretation: This study reveals that macrophage metabolic reprogramming activates HIF-1α and subsequently promotes aortic dissection progression, suggesting that macrophage HIF-1α inhibition might be a potential therapeutic target for treating aortic dissection.

1. Introduction

Aortic dissection is an aggressive vascular disease with high mortality and poor prognosis [1,2]. Usually, aortic dissection is initiated by an intimal tear, which further results in blood flow into

☆ ☆**Research in context** Evidence before this study Inflammation mediated by macrophages is involved in the pathogenesis of aortic dissection, which indicates that rather than hypertension and many connective tissue disorders, local vascular inflammation may be a leading cause. Inflammation is associated with not only tissue damage but also destruction of extracellular matrix. Macrophage hypoxia-inducible factor 1-alpha (HIF-1α) promotes the pro-inflammatory phenotype switching generally. **Added value of this study** Given macrophage HIF-1α is involved in general inflammation, is macrophage HIF-1α the key point in the relative peculiar inflammation process when aortic dissection occurs? If so, what is responsible for HIF-1α activation in macrophages? Our work demonstrates that macrophages undergo robust metabolic reprogramming including changes in the level of metabolites and related enzyme in the development of aortic dissection. Of note, the accumulation of fumarate induces the overexpression of HIF-1α in macrophages. Macrophage-specific HIF-1α inhibition plays a protective role in aortic dissection formation through downregulation of a disintegrin and metallopeptidase domain 17 (ADAM17) to mitigate inflammation and inhibit degradation of extracellular matrix. **Implication of all the available evidence** Our results provide evidence that metabolic reprogramming in macrophage mitochondria contributes to the progression of aortic dissection and macrophage HIF-1α inhibition will be a beneficial strategy for treatment of aortic dissection. Acriflavine, a HIF-1α selective inhibitor, might be of great potential to protect against aortic dissection mainly by targeting macrophage HIF-1α.

* Correspondence authors.
E-mail addresses: taozhang@bjmu.edu.cn (T. Zhang), xwang@bjmu.edu.cn (X. Wang), jiangchangtao@bjmu.edu.cn (C. Jiang).
# These authors contributed equally.

https://doi.org/10.1016/j.ebiom.2019.09.041

the media layer of the aorta, leading to separation of the layers within the aortic wall [3]. Pathological features of this progression include overactivation of immune system inflammation and extracellular matrix degradation, contributing to vascular remodeling and weakening of the aortic wall [4,5]. In addition, emerging evidence indicated that genetic mutation mainly contributes to aortic dissection formation, especially a loss of function mutation in the lysyl oxidase (LOX) in humans [6]. Therefore, β-aminopropionitrile (BAPN, a LOX inhibitor)-induced aortic dissection in mice greatly resembles the process of human aortic dissection formation [7,8].

Macrophages are an essential component of the innate immune system and play a critical role in initiating further immune response by recruiting more neutrophils and monocytes/macrophages [9–12]. Normally the function of macrophages is strictly controlled. However, upon Th1 cytokine activation, these macrophages are more likely to be excessively activated and adopt a proinflammatory or M1 phenotype [13,14], which is responsible for the secretion of proinflammatory cytokines such as TNF-α, IL-6, MCP-1 and IL-10 [15] and thus contribute to the development of inflammation.

Inflammation and hypoxia are usually interdependent [16]. Hypoxia-inducible factors (HIFs), especially HIF1, are activated in response to the hypoxic and inflammatory microenvironment [17]. HIFs comprise an O_2-sensitive α subunit (HIFα) and a constitutively expressed β subunit (HIF1β) [18]. Under normoxia, HIFα is hydroxylated by prolyl hydroxylase (PHD) and subsequently conjugated by the E3 ubiquitin ligase complex containing the von Hippel-Lindau disease tumor suppressor (VHL) protein, leading to rapid degradation via the proteasome pathway. Under hypoxia, hydroxylation by PHD is inhibited, resulting in stabilization of the α subunit, dimerization with the β subunit, and hence activation of HIF target genes [19]. In most vascular diseases, the local lesion is hypoxic and infiltrated by a large number of macrophages, which suggests that macrophage HIF-1α is activated. Macrophage HIF-1α contributes to the pathogenesis of atherosclerosis by promoting lipid uptake and proinflammatory activation [20–23]. Macrophage HIF-1α was also reported to correlate with abdominal aortic aneurysm (AAA) [24]. Activation of HIF-1α by inhibiting PHD-2 had a protective effect in the development of AAA [25], and disruption of macrophage-specific HIF-1α aggravated AAA progression in mice [26]. On the other hand, HIF-1α gene silencing reduced vascular inflammation and Matrix metalloproteinase (MMP) activity to attenuate AAA [27,28]. However, the role of macrophage HIF-1α in aortic dissection remains unknown.

Given the critical role of macrophages in the inflammatory response, we demonstrated that macrophages undergo robust metabolic reprogramming, especially the accumulation of intracellular fumarate, leading to HIF-1α activation in the pathogenesis of aortic dissection. Furthermore, activation of HIF-1α promoted the proinflammatory response and disruption of elastic fibers by elevating the expression of the novel HIF-1α target gene *Adam17*. Our finding suggests that macrophage HIF-1α would be a viable target for aortic dissection therapy.

2. Materials and methods

2.1. Materials for experiments

β-aminopropionitrile (BAPN, A3134), Angiotensin II (Ang II, A9525) and Lipopolysaccharides (LPS, L2630) were obtained from Sigma-Aldrich (St. Louis, MO, USA). Acriflavine (HY-100575) was purchased from MCE (Monmouth Junction, NJ, USA). Thioglycollate was purchased from BD Biosciences (San Diego, CA, USA). AP-red (ZLI-9042) was purchased from ZSGB-Biotechnology Company (Beijing, China). Antibodies applied for flow cytometry were purchased from BioLegend (San Diego, CA, USA). Anti-HIF-1α (20960-1-AP, RRID: AB_10732601) antibody was purchased from Proteintech Group (Rosemont, IL, USA). Anti-ADAM17 (ab2051, RRID: AB_302796), anti-α-smooth muscle actin (ab5694, RRID: AB_2223021), anti-MMP2 (ab37150, RRID: AB_881512) and anti-MMP9 (ab38898, RRID: AB_776512) antibodies were purchased from Abcam (Cambridge, MA, USA). Anti-CD68 (MCA1957, RRID: AB_322219) antibody was purchased from Bio-Rad Laboratories (Hercules, CA, USA). Anti-β-actin (8457, RRID: AB_10950489) antibody was purchased from Cell Signaling Technology (Danvers, MA, USA). Anti-eIF5 (sc-28309, RRID: AB_627507) antibody was purchased from Santa Cruz Biotechnology (Dallas, TX, USA). The HRP-conjugated anti-rabbit IgG (sc-2004, RRID: AB_631746) and HRP-conjugated anti-mouse IgG (sc-2005, RRID: AB_631736) secondary antibodies were purchased from Santa Cruz Biotechnology (Dallas, TX, USA). Other reagents were obtained from Sigma-Aldrich (St. Louis, MO, USA) unless otherwise specified.

2.2. Animals

All animal procedures were reviewed and approved by the Institutional Animal Care and Use Committee of Peking University Health Science Center in accordance with the U.S. Department of Agriculture, International Association for the Assessment and Accreditation of Laboratory Animal Care, and National Institutes of Health guidelines. Wild-type (WT) mice on a C57BL/6J background were obtained from Vital River Laboratories (Beijing, China). The myeloid-specific HIF-1α knockout (HIF-1$\alpha^{\Delta lysm}$) and corresponding WT mice on a C57BL/6J background were generated using the Cre-loxP system. The lysozyme M (LysM) Cre recombinase was inserted into the first coding ATG of the lysozyme 2 gene (Lyz2) [29]. The HIF-1α flox (HIF-1$\alpha^{fl/fl}$) mice (RRID: MGI_3815313) were described previously [30]. LysHIF-1$\alpha^{LSL/LSL}$ mice were described in an earlier study [31,32], Oxygen-stable HIF-1α complementary DNA was expressed downstream of a loxP-stop-loxP cassette. These mice were crossed to Lys-Cre transgenic mice to overexpress HIF-1α in macrophages. Experimental mice (WT, HIF-1$\alpha^{\Delta lysm}$, HIF-1$\alpha^{fl/fl}$) at 3 weeks of age were fed a chow diet containing BAPN solution (0.5%) for 28 days or BAPN solution (0.1%) for 28 days followed by infusion with Ang II (1000 ng/kg/min) or physiological saline (0.9% sodium chloride) by Alzet osmotic pumps for 72 h (DURECT Corp, Model 2004) as described previously [33].

2.3. Cell isolation and culture

For primary mouse peritoneal macrophages, C57BL/6J mice (male, 6–8 weeks old) were injected intraperitoneally with 4% thioglycollate solution (2 mL). Three days later, peritoneal cells were harvested and incubated in RPMI-1640 medium supplemented with 10% FBS. Three hours later, nonadherent cells were removed, and the attached cell monolayer was used as peritoneal macrophages. RPMI-1640 (61870044) was obtained from Gibco (Gibco, USA).

2.4. Patients and sample processing

Aortic fragments were taken from six patients who underwent surgical repair of thoracic aortic dissection. Samples of aortic tissue were collected from two sites in each patient: the midportion of the hematoma and the transition zone between the non-dissected aorta and the proximal aspect of the hematoma. The transition zone of aortic fragment was used as the negative control. The clinical characteristics of the included patients are presented in the Table S1. The study and all experimental procedures were approved by the Ethics Committee of Peking University People's Hospital according to the Council for International Organizations of Medical Sciences. All participants were recruited from the Department of

Vascular Surgery at Peking University People's Hospital. Informed consent was obtained from all subjects.

2.5. Blood pressure measurement

For telemetry measurements, experimental mice (HIF-1$\alpha^{\Delta lysm}$, HIF-1$\alpha^{fl/fl}$) were fed a chow diet containing BAPN solution (0.5%) for 28 days. At the end of this study, the experimental mice were anesthetized with isoflurane and by implanting a telemetric blood pressure radio-transmitter (DSI, Minnesota) in left common carotid artery blood pressure was measured for 24 h [34]. These data were recorded in the physiological data acquisition and analyses system.

2.6. Recombinant adenovirus construction and infection in mice

The full-length cDNA of ADAM17 was subcloned into the adenoassociated virus serotype 2 (AAV2) vector pAV-FH (Vigene Inc., Shandong, China), and AAV2 vector pAV-C-GFP was applied as a negative control. Recombinant AAV2 plasmids were then co-transfected with Ad-helper vector and pAAV-rep/cap vector into HEK293T cells for 72 h. The supernatant was collected for further purification by PEG8000 precipitation. Purified AAV virus was applied for in *vivo* experiments.

Three-week-old male HIF-1$\alpha^{\Delta lysm}$ and HIF-1$\alpha^{fl/fl}$ mice were injected with 200 μL of AAV2-GFP or AAV2-ADAM17 virus at a titer of 1×10^{11} v.g./mL per mouse via the tail vein. BAPN was provided from the first day by injection and maintained for 4 weeks. Peritoneal macrophages were first isolated to validate the virus infection efficiency by measuring the percentage of GFP$^+$ cells by flow cytometry and the expression of ADAM17 by western blotting and real-time PCR [35].

2.7. Flow cytometry analysis

To prepare a single-cell suspension of aortic cells, the whole aorta was isolated during aortic dissection development, and the connective and fat tissues around the aorta were removed completely. The aortas were cut into pieces and digested into single cells by incubating the aorta for 60–90 min at 37 °C with 1 ml dissociation enzyme solution [36]. Final enzyme digestion solution concentration (diluted in PBS) is: Collagenase, Type I (450 U/mL), Collagenase Type, XI (125 U/mL), Deoxyribonuclease I from bovine pancreas, type II (60 U/mL), Hyaluronidase from bovine testes, type 1-s (60 U/mL). All these Collagenases were purchased from Sigma-Aldrich (St. Louis, MO, USA). Digested single-cell suspension was used for flow cytometric analysis.

To identify proinflammatory macrophages, FITC anti-CD45 (marker for leukocytes), BV421 anti-CD64 (marker for macrophages), APC anti-CD11c and PE anti-CD206 (CD11c$^+$ CD206$^-$ for proinflammatory macrophage) antibodies were used in the flow cytometry analysis. For the gating strategy, CD45$^+$ CD64$^+$cells were gated from single cells of the whole aorta, and then the percentage of CD11c$^+$ CD206$^-$ cells in CD45 CD64 double positive cells were analyzed to identify the activation of proinflammatory macrophages [37]. Cells were incubated with primary antibodies for 30 min on ice. After the unbound antibodies were washed out, labeled cells were analyzed using a BD FACS Celesta system (BD Biosciences, San Diego, CA). For analysis, During the flow cytometry analysis, we collected almost all the cells for each sample (single cells from a whole aorta). More than 600,000 cells were collected and the number of CD45$^+$cells exceeded 5000. The data were analyzed by using Cell Quest (BD Biosciences, San Diego, CA, USA) or FlowJo (Tree Star Inc., Ashland, OR, USA).

2.8. Enzyme-linked immunosorbent assay (ELISA)

The levels of mouse TNF-α and fumarase were measured via ELISA kits (Cat. EM008, Cat. F10703-B for murine) according to the manufacturer's instruction. The TNF-α ELISA kit was purchased from ExCell Bio (Shanghai, China). The fumarase ELISA kit was purchased from Biological (Beijing, China). Briefly, standards or samples were added into the plate provided by the ELISA kits. After incubation at 37 °C for 90 min, biotin-conjugated antibody solution, avidin-HRP solution, TMB substrate solution and stop solution were added to each well step by step. Absorbance at 450 nm was measured within 15 min.

2.9. Cytometric bead array (CBA)

The level of inflammatory cytokines in plasma was measured using a cytometric bead array mouse inflammation kit (Cat. 552364, BD Biosciences, San Jose, CA, USA) according to the manufacturer's instructions.

2.10. ADAM17 enzymatic activity assay

An ADAM17 activity assay was performed on the basis of cleavage of fluorescent substrate. Macrophage protein lysate was extracted using a lysis buffer with high enrichment of membrane-bound proteins and Mca-Pro-Leu-Ala-GlnAla-Val-Dpa-Arg-Ser-Ser-Ser-Arg-NH2 fluorogenic peptide substrate III (R & D Systems, ES003) was used as the substrate for ADAM17. The ADAM17 activity assay by R & D Systems was carried out according to the manufacturer's instructions. A total amount of 5 μg protein was used for ADAM17 enzymatic activity assay, and the assay was run as a kinetic assay mode for 24 h [38].

2.11. Quantitative PCR (qPCR)

Total RNA was isolated using TRIzol reagent (Cat. 15596018, Thermo Fisher Scientific, Waltham, MA, USA). Total RNA (2 μg) was reverse transcribed into cDNA using 5X All-In-One RT MasterMix (Cat. G490, abm, Richmond, BC, Canada). The qPCR analysis was performed with RealStar Green Power Mixture (Cat. A314, GenStar, Beijing, China) and recorded in an Mx3000 Multiplex Quantitative PCR System (Agilent, La Jolla, CA, USA). The amount of PCR product in each cycle was evaluated by the fluorescence intensity of SYBR Green I. The results were analyzed using Stratagene Mx3000 software, and the target mRNA levels were normalized to the level of Actb mRNA. The primer sequence information is included in Table S2.

2.12. Western Blot

Tissues or cells were lysed in RIPA lysis buffer (Cat. P0013C, Beyotime Biotechnology, Shanghai, China). Equal amounts of protein were subjected to sodium dodecyl sulfate polyacrylamide gel electrophoresis on a 10% or 8% running gel and then transferred to a polyvinylidene fluoride membrane. The membrane was incubated with 10% BSA in Tris Tween-buffered saline at room temperature for 1 h, with different primary antibodies at 4 °C for 12 h and with an appropriate horseradish peroxidase (HRP)-conjugated secondary antibody for 1.5 h at room temperature. The bands were detected with the ChemiDOC XRS System (Bio-Rad, Hercules, CA, USA).

2.13. Chromatin immunoprecipitation (ChIP)

Chromatin immunoprecipitation (ChIP) was performed using macrophages as described previously [17]. Isolated peritoneal macrophages were fixed in formaldehyde for 10 min and then

quenched with glycine. The cells were collected, and the chromatin DNA was sheared to fragments (approximately 100–300 bp) using the M220 Focused-ultrasonicator (Covaris, Woburn, MA, USA). The samples were incubated with anti-HIF-1α (Cat. sc-10790, RRID: AB_2116990, Santa Cruz Biotechnology, Dallas, TX, USA) or anti-IgG (Cat. sc-2027, RRID: AB_737197, Santa Cruz Biotechnology, Dallas, TX, USA) antibody (2 μg) in ChIP lysis buffer containing bovine serum albumin (BSA) (1 μg/mL). Protein A/G plus-agarose beads (Cat. sc-2003, RRID: AB_10201400, Santa Cruz Biotechnology, Dallas, TX, USA) were prepared, added to the samples and incubated overnight at 4 °C. The beads were washed with ChIP wash buffer four times. The DNA fragments were eluted by ChIP elution buffer and purified by phenol-chloroform-isoamyl alcohol before precipitation with glycogen, NaAc (pH = 5.2) and ethanol overnight. The DNA fragments were suspended in ultrapure water and quantitated by quantitative PCR (qPCR) analysis. The primer sequence information is included in Table S3.

2.14. Seahorse extracellular flux analysis

The Seahorse XF24 Extracellular Flux Analyzer was used to measure the metabolic conditions of murine peritoneal macrophages. Cells were plated at 5×10^4 cells/well in 24-well XF microplates and cultured for 6 h. RPMI-1640 medium was replaced with XF base medium supplemented with 25 mM glucose and 2 mM pyruvate. After incubation in CO_2-free conditions for one hour at 37 °C, the oxygen consumption rate (OCR) and extracellular acidification rates (ECAR) were measured following the manufacturer's instruction. Mitochondrial stress tests were performed under basal conditions or with metabolic reagents, including 1 mM oligomycin, 1 mM FCCP, 1 mM rotenone, and 1 mM antimycin A. The ECAR was calculated by Wave software.

2.15. Histological, immunohistochemical, and immunofluorescence analysis

Histological staining of the same region of the harvested thoracic aorta was performed to obtain morphometric data using a standardized protocol as previously described [39]. Human and mouse aortic tissues were divided into (spaced 0.5-mm apart) 7-μm-thick serial sections. Human and mouse aortic sections were stained with primary antibodies against HIF-1α (Cat. 20960-1-AP, RRID: AB_10732601, Proteintech, Rosemont, IL, USA) and CD68 (Cat. MCA1957, RRID: AB_322219, Bio-Rad Laboratories, Hercules, CA, USA) followed by fluorescent secondary antibodies (Alexa Fluor 488/546 goat anti-rabbit/rat IgG) for immunofluorescence analysis. All histological analyses were performed at room temperature using a Leica Microsystems instrument (Fluorescence Light DM4000B and Confocal TCS SP8 Microscopes). Mouse thoracic aortic tissues were divided into (spaced 0.5-mm apart) 7-μm-thick serial sections and analyzed by Verhoeff-Von Gieson staining for elastin assessment. Elastin degradation was graded on a scale of 1–4, where 1 indicates<25% degradation, 2 indicates 25 to 50% degradation, 3 indicates 50 to 75% degradation, and 4 indicates >75% degradation [33,40]. The data were evaluated by two blinded independent investigators and presented as the mean of serial sections for each mouse.

2.16. In situ zymography

MMP (matrix metalloproteinase) activity was detected in thoracic aorta using EnzChek Gelatinase/Collagenase Assay Kit (E12055, Invitrogen, Waltham, MA) according to the manufacturer's instruction. Experimental mice (WT, HIF-1$\alpha^{\Delta lysm}$, HIF-1$\alpha^{fl/fl}$) at 3 weeks of age were fed a chow diet containing BAPN solution (0.5%) for 28 days. After perfusion with PBS and dissection, Mouse aortic tissues were divided into (spaced 0.5-mm apart) 7-μm-thick serial sections, and serial sections for each thoracic aorta were incubated with DQ gelatin for 1 h Images of the tissues were obtained using a Leica Microsystems instrument (Fluorescence Light DM4000B and Confocal TCS SP8 Microscopes). The data were evaluated blindly by 2 independent investigators and presented as the mean of serial sections for each aorta [41].

2.17. Metabolomics analysis

Analysis of metabolites was performed with liquid chromatography-tandem mass spectrometry (LC-MS/MS). For metabolite extraction, cultured cells were washed with saline twice, lysed in 80% aqueous methanol (v/v) and equilibrated at −80 °C for 20 min. Glutamine was added as an internal standard. Cells were oscillated for 10 min and centrifuged at a speed of 14,000 g for 10 min at 4°C. Cell supernatants of metabolite extracts were collected, dried, and stored at −80 °C before injection. For LC-MS/MS analysis, samples were reconstituted in water and analyzed using a QTRAP 5500 LC-MS/MS system (AB SCIEX) coupled with an ACQUITY UHPLC System (Waters Corporation). An Xbridge Amide column (100×4.6 mm i.d., 3.5 Lm; Waters Corporation) was employed for compound separation at 30 °C. Mobile phase A was 5 mM ammonium acetate in water with 5% acetonitrile, and mobile phase B was acetonitrile. The linear gradient used was as follows: 0 min, 90% B; 1.5 min, 85% B; 5.5 min, 35% B; 10 min, 35% B; 10.5 min, 35% B; 14.5 min, 35% B; 15 min, 85% B; and 20 min, 85% B. The flow rate was 0.5 ml/min. MultiQuant v3.0 software (AB SCIEX) was used to process all raw LC-MS/MS data and integrate chromatographic peaks. Integrated peak areas corresponding to metabolite concentrations were further analyzed using the MetaboAnalyst website (http://www.metaboanalyst.ca). Metabolite abundance was expressed relative to the internal standard.

2.18. Statistical analysis

Data analyses were performed using Prism version 8.0 (GraphPad Software, San Diego, CA, USA) and IBM SPSS 24.0 (IBM Corporation, Armonk, NY). Normal distribution of the data was assessed using the Shapiro Wilk test. The unpaired 2-tailed Student *t*-test was performed to analyze two groups for significant differences. One-way ANOVA and least significant difference post hoc tests were used to evaluate the statistical significance of differences between more than two groups. For the nonparametric tests, the two-tailed Mann-Whitney U test (comparison between two groups) and Kruskal-Wallis test (comparison between three or more groups) followed by a Dunn's post hoc analysis were used to evaluate statistical significance. All results are expressed as mean ± SEM. The significance level was set at $^*P < 0.05$.

3. Results

3.1. Macrophage HIF-1α expression is upregulated in the aorta of both patients and mouse models with aortic dissection

To investigate the involvement of macrophages, we examined the expression of CD68 (biomarker of macrophages) in proximal aortic tissue from aortic dissection patients with hematoma and nondissected controls. We found that $CD68^+$ macrophages were predominantly localized in the lesion of the thoracic aorta (Fig. 1a). In most vascular diseases, the local lesion is hypoxic, and therefore, we assessed HIF-1α expression in the intimal and medial regions of thoracic aortas from patients with aortic dissection. Compared to control aortic arteries, the focal zone of aortic dissection specimens revealed notably higher expression of HIF-1α in infiltrating macrophages (Fig. 1b). In vivo, two mouse models were

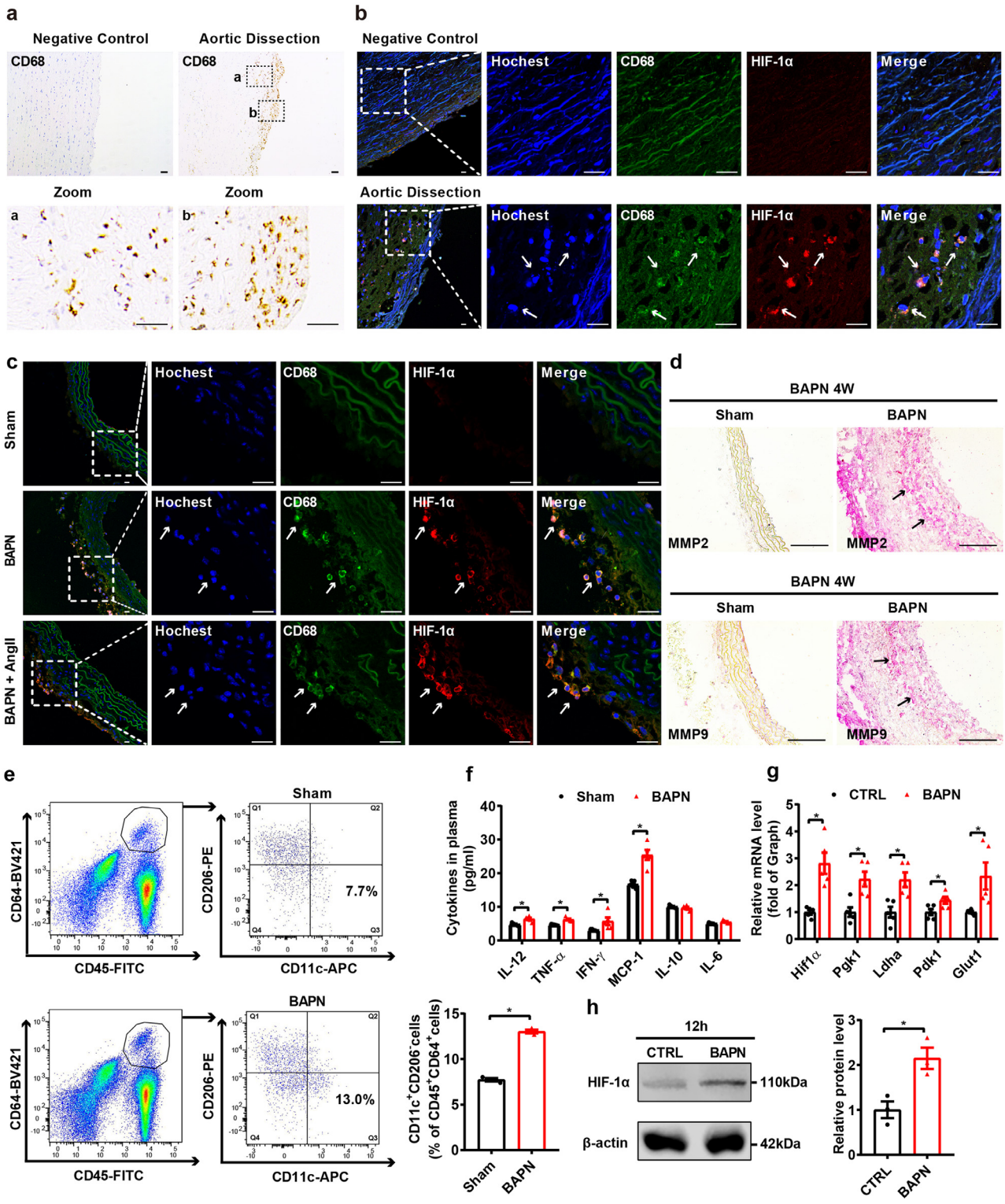

Fig. 1. Macrophage HIF-1α signaling is activated in the aorta of aortic dissection patients and mice with hematoma.
(a) Immunohistochemical staining for macrophages (CD68) in transverse cryosections of aortas from patients with aortic dissection ($n = 6$). Scale bar, 50 μm.
(b, c) Immunofluorescence staining for macrophages (CD68, green) and HIF-1α (red) in transverse cryosections of aortas from patients with aortic dissection (b, $n = 6$) and sham-, BAPN-treated and BAPN+Ang II-treated mice (c, $n = 6$). Nuclei were stained with Hoechst (blue), and elastin (autofluorescence) appears green. Scale bar, 25 μm.
(d) Immunohistochemical staining for MMP2 (red) and MMP9 (red) in transverse cryosections of aortas from sham and BAPN-treated mice ($n = 3$). Scale bar, 100 μm.
(e) Quantification of the percentage of $CD11c^+/CD206^-$ proinflammatory macrophages among $CD64^+$ $CD45^+$cells (macrophages) in aorta from sham- and BAPN-treated mice ($n = 3$).
(f) CBA analysis of plasma inflammatory cytokine levels in plasma from sham- and BAPN-treated C57BL/6 J mice ($n = 5$).
(g) qPCR analysis of *Hif1α*, *Pgk1*, *Ldha*, *Pdk1*, and *Glut1* (HIF-1α target genes) mRNA levels in BAPN (1.2 mM, 12 h)-treated peritoneal macrophages ($n = 5$).
(h) Representative western blots and quantification for HIF-1α in vitro ($n = 3$).
The data are presented as the mean ± SEM. Student's unpaired *t*-test was used for comparisons between two groups (e-h). Statistical significance is indicated by $^*P < 0.05$, compared with sham (e-f). $^*P < 0.05$ compared with the control group (g-h).

used to validate the clinical process of aortic dissection. Three-week-old C57BL/6 mice were administered β-aminopropionitrile (BAPN, 0.5%) only for 4 weeks or low-dose BAPN (0.1%) for 4 weeks followed by angiotensin II (Ang II, 1000 ng/kg/min) infusion for 72 h. Administration of BAPN and BAPN/Ang II both led to a disrupted elastic plate and severe aortic dissection [7] (Fig. S1a-c). Consistent with human tissues, aortas from two aortic dissection animal models showed more infiltrating macrophages and markedly higher HIF-1α levels in macrophages than those of controls (Fig. 1c, Fig. S1d). Matrix metalloproteinase 2 (MMP2) and matrix metalloproteinase 9 (MMP9) were reported to induce the degradation of extracellular matrix proteins during the development of a dissecting aneurysm [42]. Immunohistochemical staining showed that MMP2 and MMP9 levels were increased in aortas from a BAPN-induced aortic dissection model (Fig. 1d). In situ zymography was used to quantify BAPN-mediated effects in the aorta, with BAPN-treatment MMP activity was increased compared with that of sham aorta (Fig. S1e). HIF-1α activation was reported to be involved in macrophage M1 polarization; thus, we performed flow cytometric analysis, gating by CD45, CD64, CD11c and CD206 expression, to assess macrophage polarization. The percentage of $CD11c^{+}/CD206^{-}$ proinflammatory macrophages in $CD64^{+}CD45^{+}$ cells was elevated in aortas from mice treated with BAPN (0.5%) for 2 weeks, indicating that more macrophages were polarized to the proinflammatory M1 phenotype in aortas with aortic dissection progression (Fig. 1e and Fig. S1f). In accordance with HIF-1α activation and the proinflammatory phenotype of infiltrating macrophages, the plasma levels of proinflammatory cytokines, such as IL-12, TNF-α, IFN-γ and MCP-1, were substantially upregulated after a 4-week BAPN treatment (Fig. 1f). To further confirm the activation of HIF-1α, we treated peritoneal macrophages with BAPN (1.2 mM) for 12 h in vitro. BAPN stimulation induced the activation of HIF-1α signaling, as well as upregulation of the mRNA expression of proinflammatory M1 marker genes such as *Il-1β*, *Tnf-α* and *Mcp-1*, and downregulation of the mRNA expression of anti-inflammatory M2 marker genes such as *Il-10*, *Arg-1* and *Cd206* in macrophages (Fig. 1g, h and Fig. S1g). Ang II is another independent risk factor for inducing aortic dissection, which has been reported to stimulate HIF-1α expression in tumor cells [43]. To further confirm the activation of HIF-1α, we treated peritoneal macrophages with Ang II (1 μM) for 12 h in vitro. Similar to what was observed in BAPN stimulation, Ang II activated the HIF-1α signaling pathway and elevated the mRNA levels of proinflammatory genes, such as *Inos, Tnf-α and Il-6*, in mouse macrophages (Fig. S2a-c). These results indicate that HIF-1α signaling is activated in macrophages infiltrating the aorta in both patients and mouse models with aortic dissection.

3.2. BAPN and Ang II promotes macrophage metabolic reprogramming and HIF-1α activation

Metabolic reprogramming plays a critical role in the phenotypic and functional switching of macrophages [44,45]. To investigate whether macrophage metabolic reprogramming was required in aortic dissection, we measured the metabolic parameters of peritoneal macrophages cultured in vitro with or without 1.2 mM BAPN for 12 h. The basal and maximal extracellular acidification rate (ECAR) were increased in BAPN-treated peritoneal macrophages compared to that of control group (69.92 ± 0.91 versus 97.31 ± 4.00 mpH/min for basal ECAR, 61.68 ± 3.51 versus 92.21 ± 1.82 mpH/min for maximal ECAR), with no change in oxygen consumption rate (OCR) and a lower ratio of OCR to ECAR (Fig. 2a, b). These data indicate that BAPN promotes dramatic metabolic reprogramming, enhances glycolytic metabolism and impairs mitochondrial oxidative phosphorylation (OXPHOS) in macrophages. To further explore the detailed changes in metabolic pathways and the possible metabolites involved, metabolites were extracted from peritoneal macrophages stimulated with or without BAPN (1.2 mM) for 12 h and analyzed by using ultra-performance liquid chromatography-coupled time-of-flight mass spectrometry (UPLC-ESI-QTOFMS) metabolite profiling. Pathway analysis showed an apparent disparity in glycolysis and the tricarboxylic acid cycle (TCA) cycle (Fig. 2c). Further analysis demonstrated that BAPN-induced macrophages had higher levels of several glycolytic intermediates, including G6P (glucose 6-phosphate), GADP (glyceraldehyde-3-phosphate), 3PG (3-phosphoglycerate), DPG (2, 3-diphosphoglycerate) and lactate, than control (Fig. 2d). TCA cycle intermediates play a key role in HIF-1α stabilization [46-49], and levels of the metabolites fumarate and malate in BAPN-treated macrophages were increased (Fig. 2d, e). We found that the expression of fumarase, which catalyzes the reversible hydration/dehydration of fumarate to malate, in BAPN-treated macrophages was significantly inhibited in a time-dependent manner, with the lowest levels at 12 h (Fig. 2f). In contrast to the suppression of fumarase, the protein level of HIF-1α in macrophages showed an increase (Fig. 2g). To further explore the detailed changes in metabolic pathways and metabolites in AngII-induced aortic dissection progression, metabolomics analysis was also performed, showing that the expression profile of metabolites of the TCA cycle was substantially modified (Fig. S3a). Further analysis demonstrated that Ang II treatment markedly increased the levels of fumarate, succinate and malate (Fig. S3b, c). Taken together, these results suggest that BAPN and AngII promote metabolic reprograming, especially the accumulation of fumarate, and subsequently upregulate the expression of HIF-1α in macrophages.

3.3. Macrophage HIF-1α deficiency attenuates aortic dissection progression

To investigate the effect of macrophage HIF-1α in aortic dissection formation, we first compared hematoma formation and the incidence of aortic dissection between wild-type (WT) mice ($HIF\text{-}1\alpha^{fl/fl}$) and macrophage-specific HIF-1α knockout mice ($HIF\text{-}1\alpha^{\Delta lysm}$). The incidence of aortic dissection and mortality in $HIF\text{-}1\alpha^{\Delta lysm}$ mice were substantially reduced compared with those of $HIF\text{-}1\alpha^{fl/fl}$ mice (Fig. 3a, b). Of note, aortic Verhoeff-Von Gieson staining showed that $HIF\text{-}1\alpha^{fl/fl}$ mice developed more extensive elastic plate breakage and wall damage than $HIF\text{-}1\alpha^{\Delta lysm}$ mice (Fig. 3c). In addition, the expression and activity of MMP2 and MMP9 were decreased in aorta from $HIF\text{-}1\alpha^{\Delta lysm}$ mice compared with $HIF\text{-}1\alpha^{fl/fl}$ mice (Fig 3d, Fig. S4a). The mRNA expression levels of *Mif*, *Mcp-1*, and *Icam-1* in aortas were also downregulated in $HIF\text{-}1\alpha^{\Delta lysm}$ mice (Fig. 3e), and the plasma levels of IL-12, TNF-α, IFN-γ, MCP-1, and IL-6 were lower in $HIF\text{-}1\alpha^{\Delta lysm}$ mice than controls after 4 weeks of BAPN treatment (Fig. 3f), revealing a decrease in both systemic and vascular inflammation. Uncontrolled high blood pressure (hypertension) is considered to be one of the major risk factors for aortic dissection. To investigate whether macrophage HIF-1α affected the blood pressure, telemetry measurement was adopted and the results showed that there was no difference in blood pressure between $HIF\text{-}1\alpha^{fl/fl}$ mice and $HIF\text{-}1\alpha^{\Delta lysm}$ mice (Fig. 3g). In vitro, we treated peritoneal macrophages from $HIF\text{-}1\alpha^{fl/fl}$ and $HIF\text{-}1\alpha^{\Delta lysm}$ mice with BAPN (1.2 mM) for 12 h and found that the mRNA levels of the proinflammatory genes such as *Tnf-α*, *Il-1β*, *Il-6* and *Inos* were markedly reduced in $HIF\text{-}1\alpha^{\Delta lysm}$ mice (Fig. 3h). Similar results were observed for the beneficial effect of HIF-1α knockout on hematoma formation and the incidence of aortic dissection after BAPN/Ang II induction (Fig. S4b-d). Together, these results indicate that HIF-1α in macrophages increases the severity of aortic dissection dilation and vessel wall damage independent of change of blood pressure.

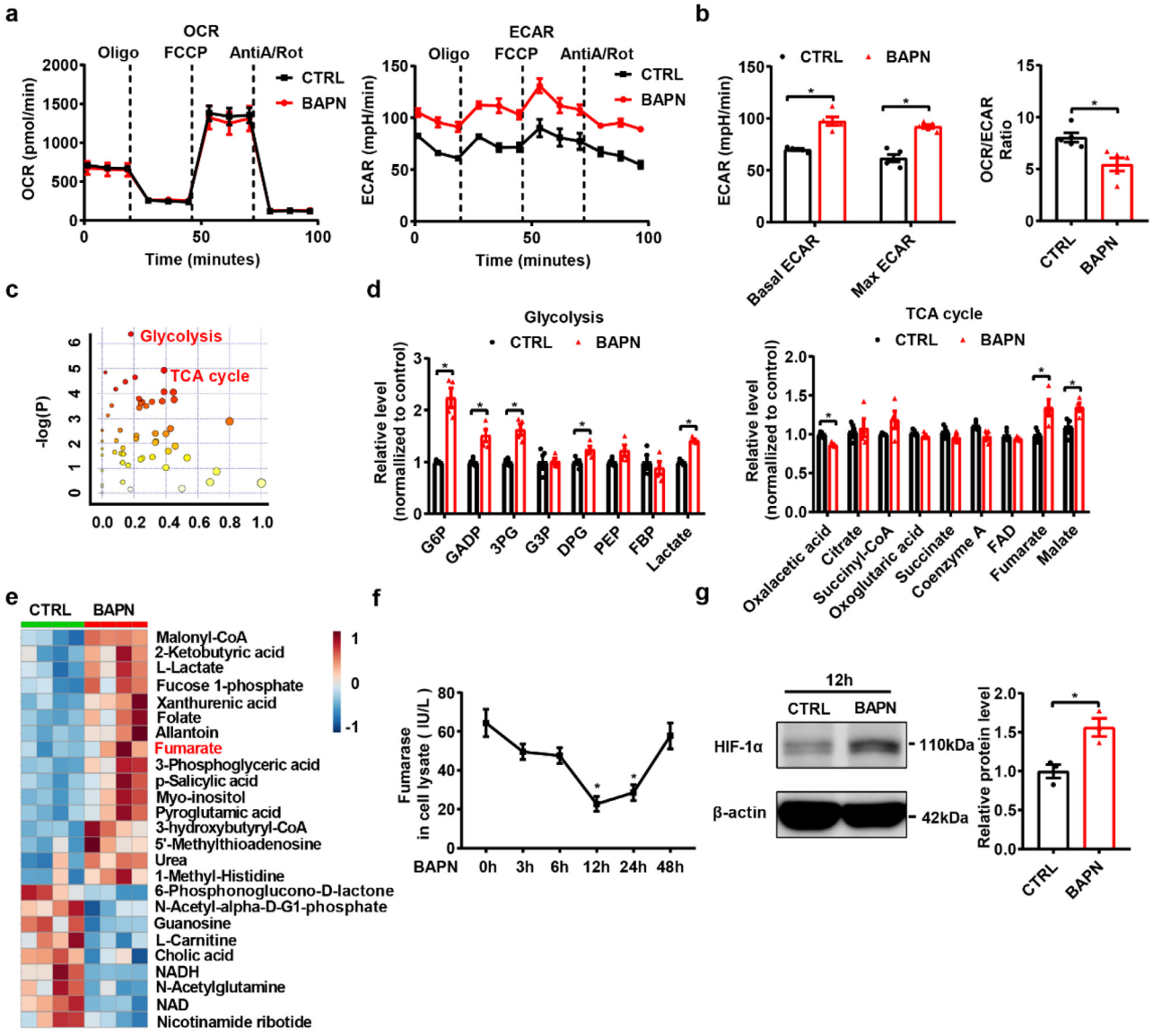

Fig. 2. BAPN bridges metabolic reprogramming and HIF-1α expression in macrophages in aortic dissection.
(a-b) Metabolic parameters of peritoneal macrophages cultured in vitro with or without 1.2 mM BAPN after 12 h ($n = 5$). The OCR and ECAR were measured at a basal level and after the injection of oligomycin, FCCP, antimycin A, and rotenone. The OCR/ECAR ratio was calculated at the basal level.
(c) Metabolic pathway analysis of peritoneal macrophages cultured in vitro with or without 1.2 mM BAPN after 12 h ($n = 4$).
(d) Relative levels of metabolites in the glycolysis and TCA cycle pathways ($n = 4$).
(e) Heatmap of the intracellular metabolites.
(f) ELISA analysis of fumarase levels in peritoneal macrophages cultured with BAPN (1.2 mM) for different durations ($n = 5$).
(g) Protein level of HIF-1α in BAPN (1.2 mM, 12 h)-treated peritoneal macrophages ($n = 3$).
The data are presented as the mean ± SEM. Student's unpaired *t*-test was used for comparisons between two groups (b, d, f, g). Statistical significance is indicated by $^{*}P < 0.05$, compared with the control group (b, d, f, g).

3.4. Macrophage HIF-1α exacerbates aortic dissection formation primarily by elevating the expression levels of the novel target gene ADAM17

To further decipher the underlying mechanism by which macrophage HIF-1α aggravates aortic dissection formation, we analyzed the interactions of 2245 HIF-1α-regulated genes obtained from the Gene Transcription Regulation Database (GTRD) with members of the ADAM or ADAMTS family, which are key regulators of extracellular matrix and vascular inflammation [38,50–52]. Three common genes (*Adamts6, Adam8, Adam17*) were analyzed (Fig. 4a), and *Adam17* expression was shown to be upregulated in macrophages after BAPN treatment, with no change in the expression of *Adamts6 and Adam8* (Fig. 4b). To directly investigate the role of HIF-1α in ADAM17 regulation in macrophages, mouse models with macrophage-specific overexpression of HIF-1α (LysHIF-1$\alpha^{LSL/LSL}$) were generated [31,32]. We found that the expression of *Adam17* was substantially upregulated in macrophages of LysHIF-1$\alpha^{LSL/LSL}$ mice compared to those of WT mice (Fig. 4c). The protein level of ADAM17 were also increased in macrophages treated with BAPN (Fig. 4d). As we know, ADAM17 is involved in cell-cell and cell-matrix interactions and function as a protease in the cleavage and ectodomain shedding of TNF-α [53]. Next, we detected the activity of ADAM17 and TNF-α secretion in each group. BAPN treatment induced increased activity of ADAM17 and secretion of TNF-α (Fig. 4e, Fig. S5a). In contrast, HIF-1α deficiency downregulated the mRNA and protein expression of ADAM17 as well as decreased ADAM17 activity and TNF-α secretion in HIF-1$\alpha^{\Delta lysm}$

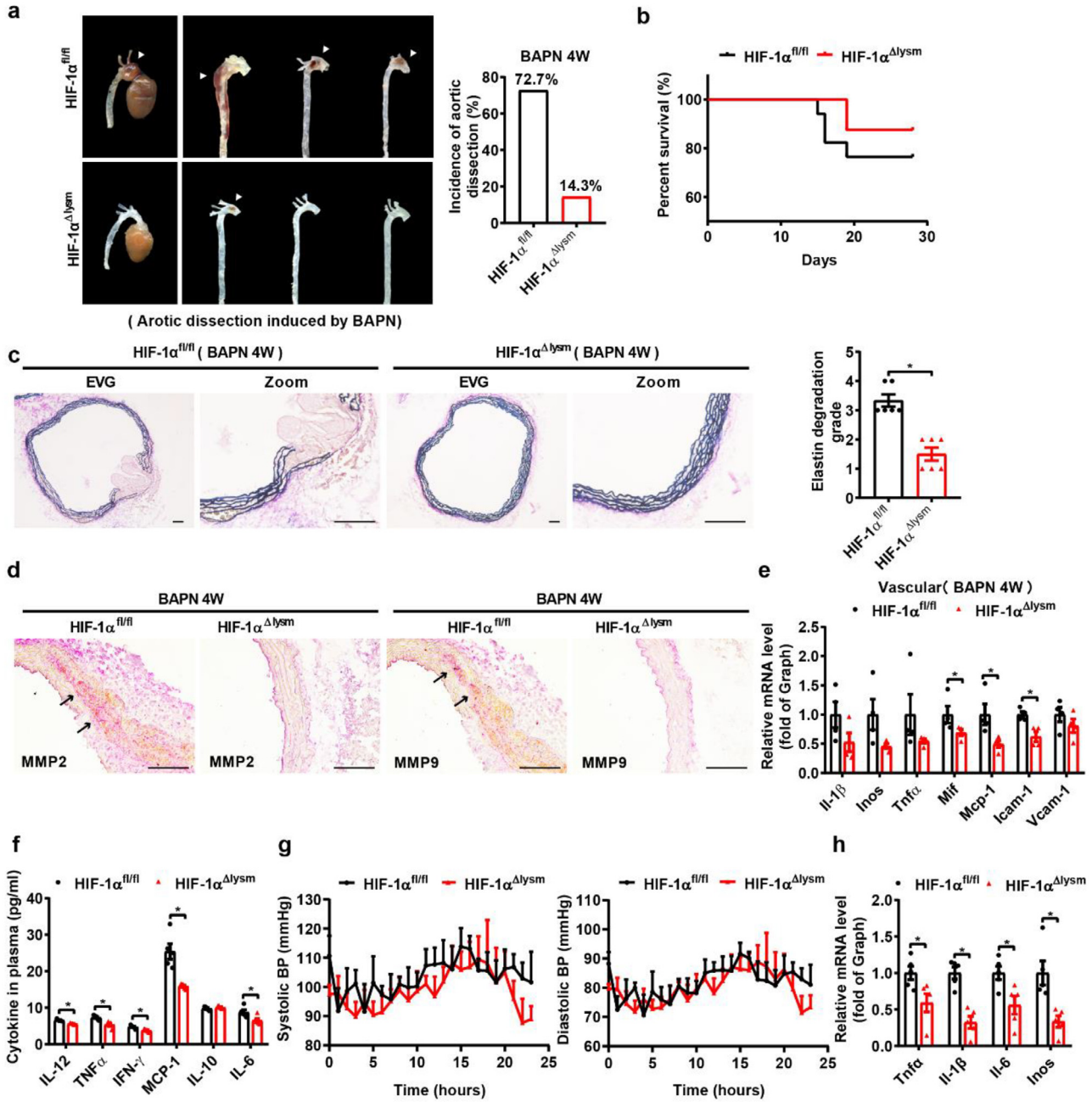

Fig. 3. The disruption of macrophage HIF-1α alleviates BAPN-induced aortic dissection development.
(a) Representative pictures of aortas obtained from HIF-1$\alpha^{fl/fl}$ and HIF-1$\alpha^{\triangle lysm}$ mice fed with BAPN (0.5%) for 28 days and aortic dissection incidence among HIF-1$\alpha^{fl/fl}$ and HIF-1$\alpha^{\triangle lysm}$ mice fed with BAPN ($n = 12$).
(b) Survival rate of HIF-1$\alpha^{fl/fl}$ and HIF-1$\alpha^{\triangle lysm}$ mice fed with BAPN ($n = 12$).
(c) Representative images of Verhoeff-Von Gieson staining of transverse cryosections of aortas from HIF-1$\alpha^{fl/fl}$ and HIF-1$\alpha^{\triangle lysm}$ mice fed with BAPN and the quantification of elastin degradation ($n = 6$). Scale bar, 100 μm.
(d) Immunohistochemical staining for MMP2 (red, $n = 3$) and MMP9 (red, $n = 3$). Scale bar, 100 μm.
(e) qPCR analysis of *Il-1β*, *Inos*, *Tnfα*, *Mif*, *Mcp-1*, *Icam1*, and *Vcam1* mRNA levels in aortas ($n = 4$).
(f) The concentration of various cytokines (IL-12, TNF-α, IFN-γ, MCP-1, IL-10, IL-6) in the plasma of BAPN-treated HIF-1$\alpha^{fl/fl}$ and HIF-1$\alpha^{\triangle lysm}$ mice ($n = 5$).
(g) Systolic and diastolic blood pressure for 24 h in HIF-1$\alpha^{fl/fl}$ and HIF-1$\alpha^{\triangle lysm}$ mice fed with BAPN for 28 days by telemetry measurements ($n = 5$).
(h) qPCR analysis of *Tnfα*, *Il-1β*, *Il-6*, and *Inos* mRNA levels in peritoneal macrophages from HIF-1$\alpha^{fl/fl}$ and HIF-1$\alpha^{\triangle lysm}$ mice treated with 1.2 mM BAPN for 12 h ($n = 5$).
The data are presented as the mean ± SEM. For the nonparametric tests, the two-tailed Mann-Whitney U test was used for comparisons between two groups (c). Statistical significance is indicated by $^*P < 0.05$, compared with HIF-1$\alpha^{fl/fl}$ mice (c); Student's unpaired *t*-test was used for comparisons between two groups (e-h). Statistical significance is indicated by $^*P < 0.05$, compared with HIF-1$\alpha^{fl/fl}$ mice (e, f, h).

macrophages (Fig. 4f–h, Fig. S5b). In vivo, aortas from two aortic dissection animal models showed more infiltrating macrophages and markedly higher ADAM17 levels in macrophages (Fig. S5c). In accordance with the data obtained from mice, the upregulated ADAM17 was shown to be colocalized with CD68 in intimal and medial regions of the thoracic aorta from patients with aortic dissection (Fig. 4i), suggesting that the expression of ADAM17 was induced in infiltrating macrophages. Protein expression and the activity of ADAM17 was markedly enhanced in macrophages with Ang II treatment (Fig. S5d-e). In addition, the increased expres-

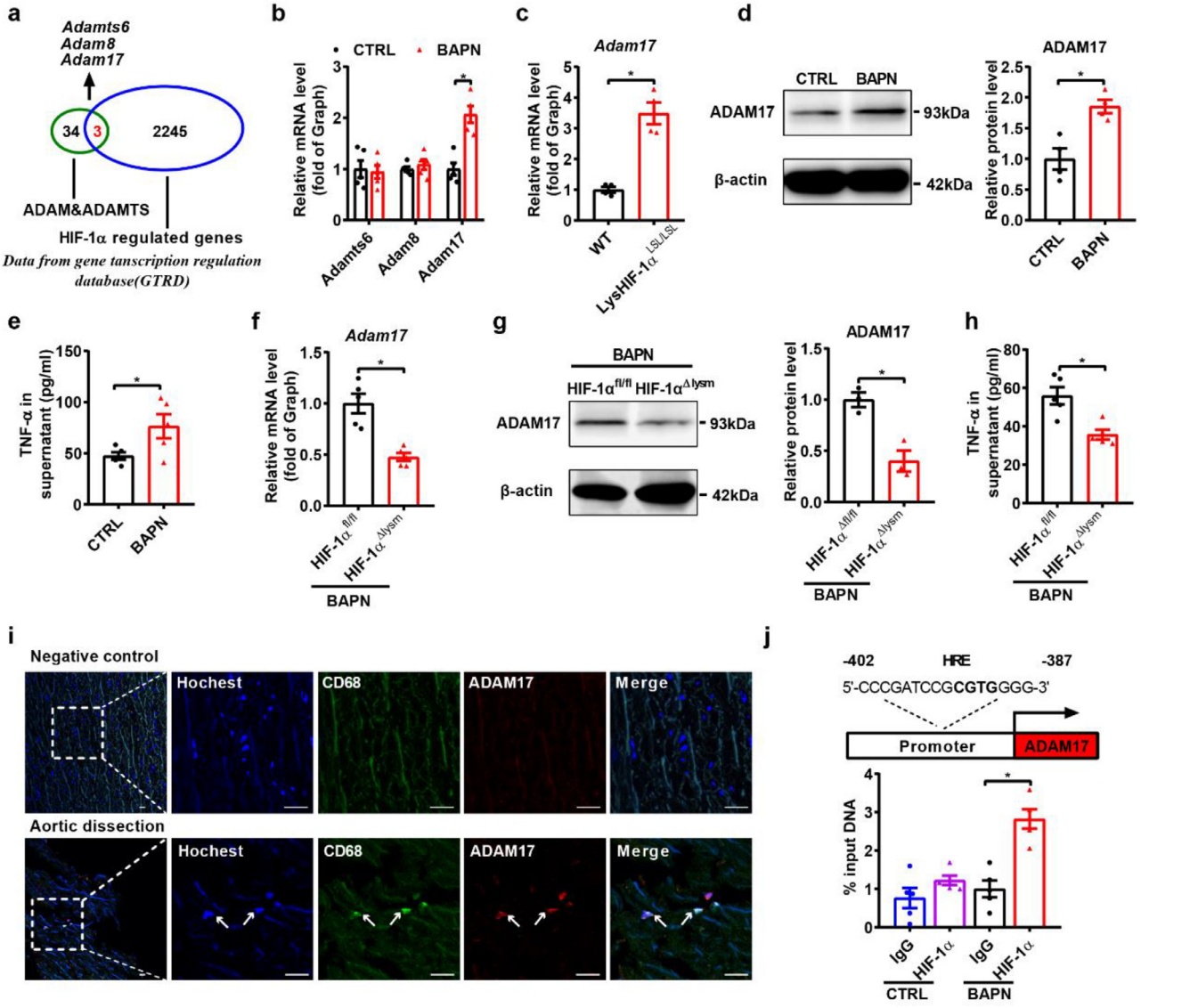

Fig. 4. ADAM17 is identified as a target gene of HIF-1α in macrophages.
(a) Venn diagram illustrating overlap between HIF-1α-regulated genes and the genes of ADAM/ADAMTS, HIF-1α-regulated genes based on the Gene Transcription Regulation Database (GTRD).
(b) qPCR analysis of *Adamts6*, *Adam8* and *Adam17* mRNA levels in BAPN (1.2 mM, 12 h)-treated peritoneal macrophages ($n = 5$).
(c) qPCR analysis of the *Adam17* mRNA level in peritoneal macrophages purified from wild-type and LysHIF-1$\alpha^{LSL/LSL}$ mice ($n = 4$).
(d) Representative western blots and quantification for ADAM17 in BAPN-treated peritoneal macrophages ($n = 3$).
(e) ELISA analysis of the supernatant TNF-α level of BAPN-treated peritoneal macrophages ($n = 4$).
(f) qPCR analysis of the *Adam17* mRNA level in peritoneal macrophages from HIF-1$\alpha^{fl/fl}$ and HIF-1$\alpha^{\triangle lysm}$ mice treated with BAPN ($n = 5$).
(g) Representative western blots and quantification for ADAM17 in peritoneal macrophages ($n = 3$).
(h) ELISA analysis of the supernatant TNF-α level of peritoneal macrophages ($n = 4$).
(i) Immunofluorescence staining for macrophages (CD68, green) and ADAM17 (red) in transverse cryosections of aortas from patients with aortic dissection ($n = 3$). Nuclei were stained with Hoechst (blue). Scale bar, 25 μm.
(j) Schematic diagram of the HRE in the murine ADAM17 gene, and chromatin immunoprecipitation (ChIP) analysis of the occupancy of ADAM17 promoter regions by *Hif1α* ($n = 5$).
The data are presented as the mean ± SEM. Student's unpaired *t*-test was used for comparisons between two groups (b-h). Statistical significance is indicated by $^*P < 0.05$, compared with the control group (b-e). $^*P < 0.05$, compared with HIF-1$\alpha^{fl/fl}$ mice (f-h); For ChIP analysis, the expression levels were normalized to the input levels; one-way ANOVA with Tukey's post hoc test (j) was performed. Statistical significance is indicated by $^*P < 0.05$, compared with IgG (j).

sion of ADAM17 and the levels of TNF-α in supernatant induced by Ang II were blunted in HIF-1$\alpha^{\Delta lysm}$ mice as well as the activity of ADAM17 (Fig S5f–h). To further explore how HIF-1α regulated ADAM17, Chromatin immunoprecipitation (ChIP) assays were performed and we found one putative HIF-1α response element (HRE) in the promoter region of ADAM17 (Fig. 4j). ChIP assay data also showed the binding of HIF-1α to the HRE of ADAM17 in the BPAN-treated macrophages (Fig. 4j). Taken together, these data suggest that ADAM17 might be a direct target gene of HIF-1α in macrophages.

We further transduced adeno-associated virus (AAV2)-green fluorescent protein (GFP) or AAV2-ADAM17-GFP into 3-week-old HIF-1$\alpha^{fl/fl}$ mice and HIF-1$\alpha^{\Delta lysm}$ mice, which were then treated by BAPN for 4 weeks (Fig. 5a). Peritoneal macrophages were isolated for detecting the efficiency of AAV infection. Flow cytometry demonstrated that 29.6% of macrophages were infected with AAV2-

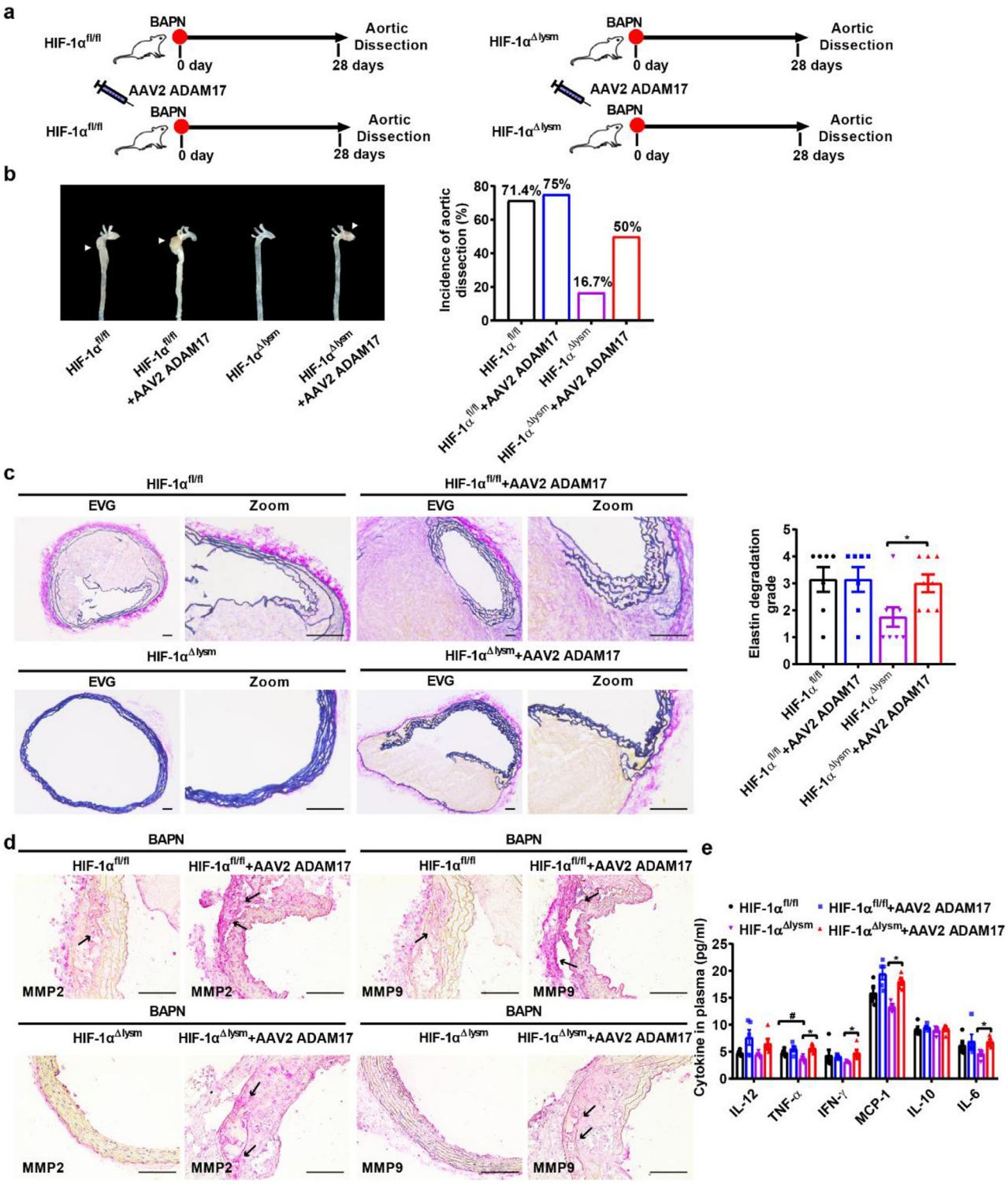

Fig. 5. Overexpression of ADAM17 reverses the protective effects of macrophage HIF-1α deficiency on aortic dissection development.
(a-b) Schematic of the experimental procedures and representative pictures of aortas obtained from HIF-1$\alpha^{fl/fl}$ and HIF-1$\alpha^{\Delta lysm}$ mice; Aortic dissection incidence among HIF-1$\alpha^{fl/fl}$ and HIF-1$\alpha^{\Delta lysm}$ mice injected with or without AAV2 ADAM17 and fed with BAPN (0.5%) for 28 days ($n = 12$).
(c) Representative images of transverse cryosections of aortas after Verhoeff-Von Gieson staining, and the quantification of elastin degradation ($n = 6$). Scale bar, 100 μm.
(d) Immunohistochemical staining for MMP2 (red) and MMP9 (red) ($n = 3$). Scale bar, 100 μm.
(e) The concentration of various cytokines (IL-12, TNF-α, IFN-γ, MCP-1, IL-10, IL-6) in plasma of BAPN-treated HIF-1$\alpha^{fl/fl}$ and HIF-1$\alpha^{\Delta lysm}$ mice with or without injection with AAV2 ADAM17 ($n = 5$).
The data are presented as the mean ± SEM. For the nonparametric tests, Kruskal-Wallis test was used for comparisons between three or more groups (c). Statistical significance is indicated by $^{*}P < 0.05$, compared with HIF-1$\alpha^{\Delta lysm}$ mice (c); One-way ANOVA with Tukey's post hoc test (e) was performed. Statistical significance is indicated by $^{*}P < 0.05$, compared with HIF-1$\alpha^{\Delta lysm}$ mice (e). Statistical significance is indicated by $^{\#}P < 0.05$, compared with HIF-1$\alpha^{fl/fl}$ mice (e).

GFP (Fig. S6a). The overexpression of ADAM17 in macrophages after AAV2-ADAM17 infection was validated by qPCR and western blot (Fig. S6b,c). ADAM17 overexpression markedly reversed the improvement in aortic dissection dilation and incidence in HIF-1$\alpha^{\Delta lysm}$ mice compared to that in HIF-1$\alpha^{fl/fl}$ mice (Fig. 5b). The beneficial effects of HIF-1α disruption in macrophages on aortic dissection were reversed by ADAM17 overexpression (Fig. 5b). Aortic Verhoeff-Von Gieson staining showed that the macrophage-specific HIF-1α ablation-mediated improvement in elastic plate breakage and wall damage was completely abrogated by ADAM17 overexpression (Fig. 5c). Immunohistochemical staining showed that the decrease in MMP2 and MMP9 expression induced by HIF-1α knockout in aortas was also blunted by ADAM17 overexpression (Fig. 5d). Similar results were obtained regarding the levels of proinflammatory cytokines in mouse plasma. Collagen-binding activity (CBA) assay indicated that increased expression of ADAM17 attenuated the BAPN treatment-augmented systemic inflammation regardless of HIF-1α deficiency (Fig. 5e). Taken together, these results suggest that ADAM17 mediates macrophage HIF-1α-induced aortic dissection formation.

3.5. Administration of a selective pharmacological HIF-1α inhibitor acriflavine suppresses aortic dissection formation in a macrophage HIF-1α-dependent manner

Given the important role of macrophage HIF-1α in the development of aortic dissection, we used a HIF-1α-selective inhibitor acriflavine [54] to determine whether targeting HIF-1α can prevent aortic dissection formation. We administered vehicle or acriflavine (2 mg/kg daily) to BAPN-treated HIF-1$\alpha^{fl/fl}$ and HIF-1$\alpha^{\Delta lysm}$ mice (Fig. 6a). Administration of acriflavine substantially suppressed the severity of aortic dissection dilation and aortic wall damage as well as the incidence of aortic dissection in HIF-1$\alpha^{fl/fl}$ mice, but there was no change in the HIF-1$\alpha^{\Delta lysm}$ mice (Fig. 6b). Verhoeff-Von Gieson staining indicated that elastin lamellae structure disruption and fiber degradation were markedly restored in acriflavine-treated HIF-1$\alpha^{fl/fl}$ mice; however, HIF-1$\alpha^{\Delta lysm}$ mice were unresponsive to acriflavine treatment (Fig. 6c). These results indicate that acriflavine treatment ameliorates aortic dissection mainly by inhibiting macrophage HIF-1α signaling. Taken together, these data support our notion that macrophage metabolic reprogramming aggravates aortic dissection through the HIF1α-ADAM17 pathway (Fig. 6d).

6. Discussion

Aortic dissection is associated with the degeneration of collagen and elastin not only as a result of the dysregulation of vessel smooth muscle cells, but also the dysregulation of immune cells [55,56]. Despite evidence of the involvement of several distinct immune cells, evidence that the metabolic state of macrophages plays a pivotal role in the development of aortic dissection remains elusive. Here, we showed that metabolic reprogramming in macrophages plays an essential role in HIF-1α activation, resulting in elevated expression of its downstream novel target gene ADAM17 and further the development of vascular inflammation.

Our findings that macrophage metabolic remodeling is coupled with the development of aortic dissection has raised several questions. First and fundamentally, are the animal models used in the present study canonical? BAPN is commonly used in mice to induce aortic dissection in a manner that is similar to the clinical process of aortic dissection development, including the process of intimal injury, hemorrhage or even rupture of the aortas. Aortic dissection is common in patients with a history of high blood pressure, but BAPN administration alone caused only a minor change in blood pressure. In consideration of this phenomenon, we employed another animal model, namely, BAPN treatment in combination with Ang II to replicate the hemodynamics in aortic dissection formation. Both animal models share the characteristics of aortic dissection in patients. Therefore, the two aortic dissection models are appropriate for the study of aortic dissection formation.

Interestingly, our data showed that the levels of some TCA metabolites, such as fumarate and/or succinate, were substantially increased after BAPN or Ang II stimulation. Our previous work and recent studies have demonstrated that macrophage HIF-1α overexpression leads to enhanced glycolytic metabolism and impaired OXPHOS [57–59]. In accordance with our previous reports, we also found herein that HIF-1α disruption in macrophages showed upregulation of OXPHOS metabolism and decreased glycolysis levels. Regarding HIF-1α activation in our models, the increase in glycolytic metabolism induced by BAPN or Ang II is supposed to be the downstream effect of HIF-1α activation, guaranteeing macrophages to accommodate the functional repertoire. However, the second change in metabolic state marked by the accumulation of some TCA metabolites, especially fumarate and/or succinate, seemed to contradict the impairment of OXPHOS induced by HIF-1α activation, suggesting that these elevated metabolites may not be regulated by HIF-1α. It is reported that some TCA cycle metabolites are responsible for the regulation of PHD activity and thus activate HIF-1α [60]. In renal cancer cells, dominant negative mutations in fumarase, which causes the elevation of intracellular fumarate, are accompanied by HIF upregulation [61]. Succinate, as a proinflammatory metabolite, also activates HIF-1α [46]. In the present study, we found that both BAPN and Ang II triggered the accumulation of fumarate in macrophages, while Ang II increased the level of succinate. Furthermore, the activity of fumarase was decreased, consistent with the elevation in intracellular fumarate and upregulation of HIF-1α. α-ketoglutarate (α-KG) is reported to increase PHD activity and deplete HIF-1α as an anti-inflammatory mediator [49]. BAPN and Ang II have little effect on changes in α-KG levels. Additionally, the levels of other TCA metabolites showed no differences on the cellular level, suggesting that other metabolites involved in the TCA cycle are not related to the activation of HIF-1α in our models. These findings suggested that macrophage metabolic remodeling induced by BAPN or Ang II is mediated mainly by the accumulation of fumarate, which acts as the upstream regulator of HIF-1α, promoting its expression and activation. Although there are some differences between the two kinds of aortic dissection models, both models exhibited elevation of the fumarate level and the pathway node HIF-1α as well as its downstream pathway, highlighting that HIF-1α in macrophages plays a key role in the development of aortic dissection.

Although inflammation is now considered to be one of the factors for aortic dissection, the role of macrophage in the development of aortic dissection remains unclear. Our study first found that macrophage HIF-1α played an important role in pathogenesis of aortic dissection. Macrophage HIF-1α knockout mice showed decreased local and systemic inflammation and improved elastic plate breakage. Moreover, ADAM17 was identified as a novel target gene of HIF-1α, and was responsible for maturity of TNF-α, which was reported to show time-dependent increase in the course of aortic dissection and may somehow be used to indicate the decrease in biomechanical strength of the involved aorta in aortic dissection [62]. More than inflammation regulation, macrophage HIF-1α-ADAM17 axis was involved in regulating the expression and activities of MMP2 and MMP9 to affect extracellular matrix degradation. So, targeting macrophage HIF-1α to improve the inflammation and destruction of the vessel wall should be a beneficial strategy for aortic dissection.

ADAM17 is reported to have a heterogeneous functional repertoire, and it remains unknown whether macrophage ADAM17 is

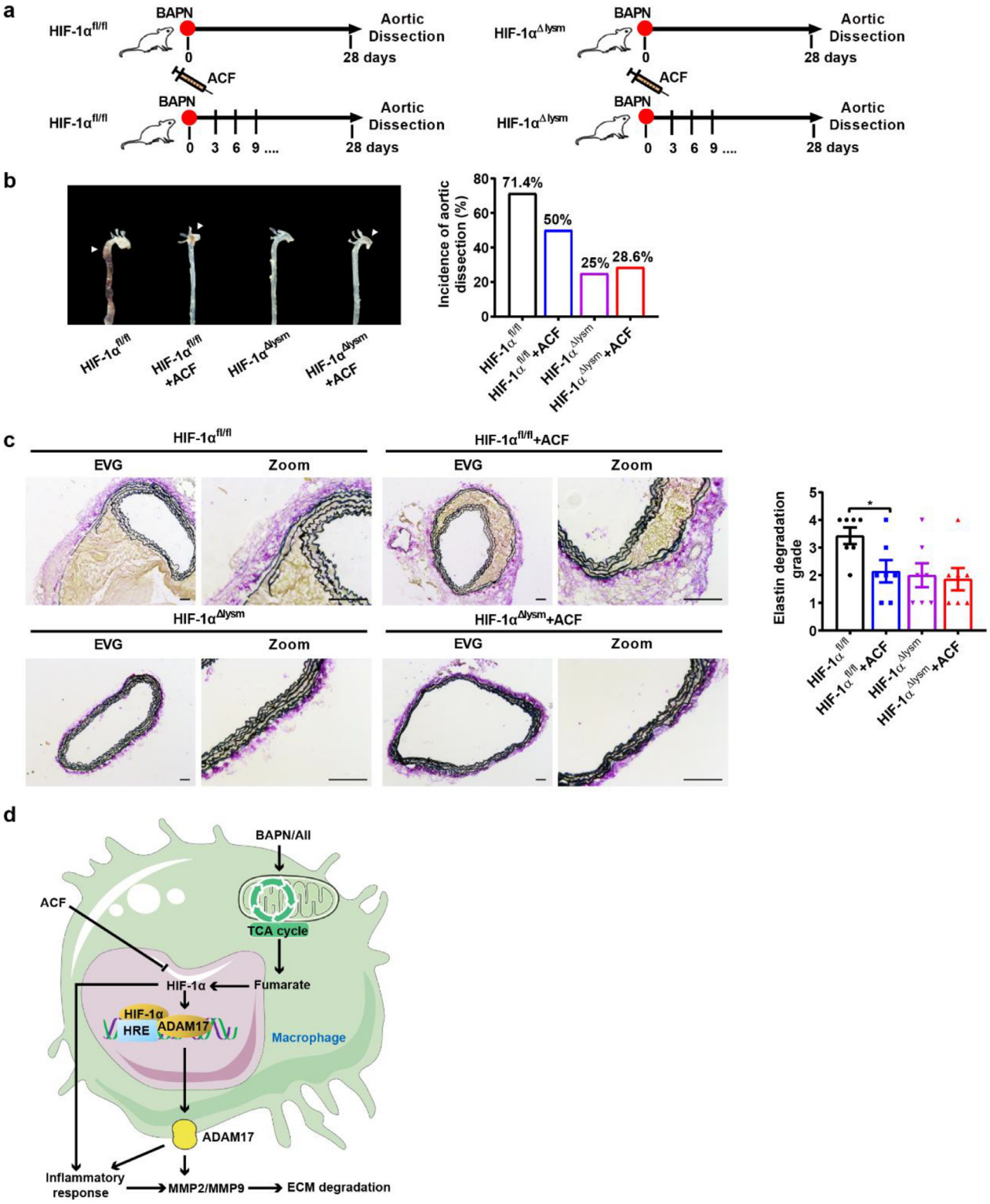

Fig. 6. Acriflavine treatment ameliorates aortic dissection formation via the inhibition of HIF-1α in macrophages.
(a-b) Schematic of the experimental procedures and representative pictures of aortas obtained from HIF-1$\alpha^{fl/fl}$ and HIF-1$\alpha^{\triangle lysm}$ mice ($n = 12$); Aortic dissection incidence among HIF-1$\alpha^{fl/fl}$ and HIF-1$\alpha^{\triangle lysm}$ mice injected with and without acriflavine (every 3 days) and fed with BAPN (0.5%) for 28 days ($n = 12$).
(c) Representative images of transverse cryosections of aortas after Verhoeff-Von Gieson staining, and the quantification of elastin degradation ($n = 6$). Scale bar, 100 μm.
(d) Schematic view of macrophage HIF-1α regulating proinflammatory response and disruption of elastic fibers via a HIF1α-ADAM17 pathway during aortic dissection development.
The data are presented as the mean ± SEM. For the nonparametric tests, Kruskal-Wallis test was used for comparisons between three or more groups (c). Statistical significance is indicated by $^{*}P < 0.05$, compared with HIF-1$\alpha^{fl/fl}$ mice (c).

involved in the progression of aortic dissection. ADAM17 is typically considered a TNF-α-converting enzyme [53]. In the present study, ADAM17 was identified as the novel target gene of HIF-1α. As a result of HIF-1α activation, the expression and activity of macrophage ADAM17 was upregulated, and the level of TNF-α secretion was also increased both in vivo and in vitro. Secondary to increased TNF-α secretion, the systemic inflammation was more severe; for example, the level of proinflammatory cytokines was elevated, especially the level of MCP-1, thereby leading to more inflammatory cells infiltration into the aorta. In addition, the whole aorta showed more severe inflammation, as confirmed by the increased expression of inflammatory genes, such as *Mcp-1* and *Icam-1*, in blood vessels. Exacerbated inflammation contributes to the formation of aortic dissection. ADAM17 is also responsible for excess matrix synthesis and degradation. It was reported that upregulation of ADAM17 in smooth muscle cells (SMCs) promoted the phenotypic switching of SMC. Increased levels of ADAM17 in endothelial cell lead to impaired cell-cell adhesion and a compromised endothelial barrier [38]. BAPN or BAPN plus Ang II administration-induced severe elastic plate fracture was blunted by macrophage-specific HIF-1α knockout, which was reversed by ADAM17 overexpression in macrophages, suggesting that the macrophage HIF-1α-ADAM17 axis is also involved in matrix degradation. It is known that MMP2 and MMP9 contribute to the degradation of extracellular matrix proteins that occurs during the development of aneurysms [42]. Therefore, we investigated whether MMP2 and MMP9 also play an important role in aortic dissection models. The expression and activity of MMP2 and MMP9 were increased in the lesion of thoracic aorta following induction by BAPN. Deficiency of macrophage HIF-1α reduced the expression and activity of MMP2 and MMP9 in both BAPN or BAPN/Ang II aortic dissection models. In addition, ADAM17 overexpression further induced higher expression of MMP2 and MMP9 in both HIF-1$\alpha^{fl/fl}$ and HIF-1$\alpha^{\Delta lysm}$ mice. These results revealed that MMP2 and MMP9 are likely to be regulated by the HIF-1α-ADAM17 axis. HIF-1α was reported to induce the expression of MMP2 and MMP9 indirectly [63–65]. Moreover, ADAM17 is responsible for directly regulating the transcription of MMP2 and MMP9 through the epidermal growth factor receptor (EGFR)-mitogen-activated protein kinase/extracellular signal-regulated kinase (MEK)-extracellular-regulated kinase (ERK) pathway in tumor cells [50]. This pathway could further account for the upregulated expression of MMP2 and MMP9. The elevated level of ADAM17 expression increased the TNF-α level and systemic as well as local inflammation. Regarding induced inflammatory response, the HIF-1α-ADAM17 axis in macrophages might promote the expression of MMP2 and MMP9 in SMCs and other infiltrating cells, for example neutrophils. The observation of decreased TNF-α expression in HIF-1α knockout macrophages as well as amelioration of elastic plate damage following a decrease in the expression of ADAM17 verified ADAM17 as the target gene of HIF-1α. Therefore, the macrophage-specific HIF-1α disruption mice presented the improvement of inflammation and vascular elastic plate, mainly due to a reduction of ADAM17, as revealed.

ADAM17 has been reported to mediate angiotensin I converting enzyme 2 (ACE2) shedding in neurons [66]. To determine whether ADAM17 might influence aortic dissection by augmenting blood pressure, blood pressure was detected; however, the results showed no difference regardless of whether HIF-1α was deleted or not, which suggests that HIF-1α-ADAM17 axis might have no influence on ACE2 shedding in macrophages.

Finally, at present, effective drugs for aortic dissection therapy are not available. The present study showed that administration of the HIF-1α inhibitor acriflavine could to some extent control the formation and development of aortic dissection mainly by targeting macrophage HIF-1α. In addition, acriflavine is reported to be useful for the treatment of chronic myelogenous leukemia and type 2 diabetes [67,68].

Taken together, our data establish that metabolic reprogramming in macrophages has a pivotal role in HIF-1α-ADAM17 signaling activation and further the development of aortic dissection. Our study revealed an essential role for macrophage HIF-1α in regulating inflammation and vascular elastic plate breakage, and provided a potential therapeutic approach to treating aortic dissection.

Funding sources

This work was supported by the National Natural Science Foundation of the P. R. of China (no. 91739303, 81670413, 91857115, 81600364, and 81921001), the National Key Research and Development Program of China (2018YFA0800700) and the Fundamental Research Funds for the Central Universities: Clinical Medicine Plus X - Young Scholars Project of Peking University (PKU2018LCXQ013, PKU2019LCXQ009). The findings had no role in study design, data collection, data analysis, interpretation, writing of the report.

Declaration of Competing Interest

None declared.

CRediT authorship contribution statement

Guan Lian: Investigation, Data curation, Writing - original draft. **Xiaopeng Li:** Investigation, Data curation, Writing - original draft. **Linqi Zhang:** Investigation, Data curation. **Yangming Zhang:** Investigation, Data curation. **Lulu Sun:** Investigation, Data curation. **Xiujuan Zhang:** Investigation, Data curation. **Huiying Liu:** Investigation, Data curation. **Yanli Pang:** Investigation, Data curation. **Wei Kong:** Investigation, Data curation. **Tao Zhang:** Investigation, Data curation. **Xian Wang:** Writing - review & editing, Writing - original draft. **Changtao Jiang:** Writing - review & editing, Writing - original draft.

Acknowledgments

We would like to acknowledge Li Su, Ph.D. from Peking University medical and health analysis center for technical assistance.

Supplementary materials

Supplementary material associated with this article can be found, in the online version, at doi:10.1016/j.ebiom.2019.09.041.

References

[1] Nienaber CA, Clough RE. Management of acute aortic dissection. Lancet (London, England) 2015;385(9970):800–11.
[2] Silaschi M, Byrne J, Wendler O. Aortic dissection: medical, interventional and surgical management. Heart (British Cardiac Society) 2017;103(1):78–87.
[3] Parve S, Ziganshin BA, Elefteriades JA. Overview of the current knowledge on etiology, natural history and treatment of aortic dissection. J Cardiovasc Surg (Torino) 2017;58(2):238–51.
[4] Tieu BC, Lee C, Sun H, et al. An adventitial IL-6/MCP1 amplification loop accelerates macrophage-mediated vascular inflammation leading to aortic dissection in mice. J Clin Invest 2009;119(12):3637–51.
[5] Nienaber CA, Clough RE, Sakalihasan N, et al. Aortic dissection. Nat Rev Dis Primer 2016;2:16053.
[6] Lee VS, Halabi CM, Hoffman EP, et al. Loss of function mutation in lox causes thoracic aortic aneurysm and dissection in humans. Proc Natl Acad Sci U S A 2016;113(31):8759–64.
[7] Jiang DS, Yi X, Zhu XH, Wei X. Experimental in vivo and ex vivo models for the study of human aortic dissection: promises and challenges. Am J Transl Res 2016;8(12):5125–40.
[8] Ren W, Liu Y, Wang X, et al. beta-Aminopropionitrile monofumarate induces thoracic aortic dissection in C57BL/6 mice. Sci Rep 2016;6:28149.
[9] Koelwyn GJ, Corr EM, Erbay E, Moore KJ. Regulation of macrophage immunometabolism in atherosclerosis. Nat Immunol 2018;19(6):526–37.

[10] Gomez D, Baylis RA, Durgin BG, Newman AAC, Alencar GF, Mahan S, et al. Interleukin-1beta has atheroprotective effects in advanced atherosclerotic lesions of mice. Nat Med 2018.
[11] Da Ros F, Carnevale R, Cifelli G, et al. Targeting interleukin-1beta protects from aortic aneurysms induced by disrupted transforming growth factor beta signaling. Immunity 2017;47(5) 959–73 e9.
[12] Tabas I, Lichtman AH. Monocyte-Macrophages and t cells in atherosclerosis. Immunity 2017;47(4):621–34.
[13] Chinetti-Gbaguidi G, Baron M, Bouhlel MA, et al. Human atherosclerotic plaque alternative macrophages display low cholesterol handling but high phagocytosis because of distinct activities of the PPARgamma and LXRalpha pathways. Circ Res 2011;108(8):985–95.
[14] McLaughlin T, Ackerman SE, Shen L, Engleman E. Role of innate and adaptive immunity in obesity-associated metabolic disease. J Clin Invest 2017;127(1):5–13.
[15] Sica A, Mantovani A. Macrophage plasticity and polarization: in vivo veritas. J Clin Invest 2012;122(3):787–95.
[16] Colgan SP, Taylor CT. Hypoxia: an alarm signal during intestinal inflammation. Nat Rev Gastroenterol Hepatol 2010;7(5):281–7.
[17] Zhang SY, Dong YQ, Wang P, et al. Adipocyte-derived lysophosphatidylcholine activates adipocyte and adipose tissue macrophage nod-like receptor protein 3 inflammasomes mediating homocysteine-induced insulin resistance. EBioMedicine 2018;31:202–16.
[18] Majmundar AJ, Wong WJ, Simon MC. Hypoxia-inducible factors and the response to hypoxic stress. Mol Cell 2010;40(2):294–309.
[19] Gonzalez FJ, Xie C, Jiang C. The role of hypoxia-inducible factors in metabolic diseases. Nat Rev Endocrinol 2018.
[20] Jiang G, Li T, Qiu Y, Rui Y, Chen W, Lou Y. RNA interference for HIF-1alpha inhibits foam cells formation in vitro. Eur J Pharmacol 2007;562(3):183–90.
[21] Parathath S, Mick SL, Feig JE, et al. Hypoxia is present in murine atherosclerotic plaques and has multiple adverse effects on macrophage lipid metabolism. Circ Res 2011;109(10):1141–52.
[22] Tawakol A, Singh P, Mojena M, et al. HIF-1alpha and PFKFB3 mediate a tight relationship between proinflammatory activation and anerobic metabolism in atherosclerotic macrophages. Arterioscler Thromb Vasc Biol 2015;35(6):1463–71.
[23] Hutter R, Speidl WS, Valdiviezo C, et al. Macrophages transmit potent proangiogenic effects of oxLDL in vitro and in vivo involving HIF-1alpha activation: a novel aspect of angiogenesis in atherosclerosis. J Cardiovasc Transl Res 2013;6(4):558–69.
[24] Sano M, Sasaki T, Hirakawa S, et al. Lymphangiogenesis and angiogenesis in abdominal aortic aneurysm. PLoS ONE 2014;9(3):e89830.
[25] Watanabe A, Ichiki T, Sankoda C, et al. Suppression of abdominal aortic aneurysm formation by inhibition of prolyl hydroxylase domain protein through attenuation of inflammation and extracellular matrix disruption. Clin Sci (Lond) 2014;126(9):671–8.
[26] Takahara Y, Tokunou T, Kojima H, Hirooka Y, Ichiki T. Deletion of hypoxia-inducible factor-1alpha in myeloid lineage exaggerates angiotensin II-induced formation of abdominal aortic aneurysm. Clin Sci 2017;131(7):609–20.
[27] Erdozain OJ, Pegrum S, Winrow VR, Horrocks M, Stevens CR. Hypoxia in abdominal aortic aneurysm supports a role for HIF-1alpha and ets-1 as drivers of matrix metalloproteinase upregulation in human aortic smooth muscle cells. J Vasc Res 2011;48(2):163–70.
[28] Yang L, Shen L, Li G, Yuan H, Jin X, Wu X. Silencing of hypoxia inducible factor-1alpha gene attenuated angiotensin -induced abdominal aortic aneurysm in apolipoprotein E-deficient mice. Atherosclerosis 2016;252:40–9.
[29] Espaillat MP, Snider AJ, Qiu Z, et al. Loss of acid ceramidase in myeloid cells suppresses intestinal neutrophil recruitment. FASEB J. 2018;32(5):2339–53.
[30] Tomita S, Ueno M, Sakamoto M, et al. Defective brain development in mice lacking the Hif-Lalpha gene in neural cells. Mol. Cell. Biol. 2003;23(19):6739–49.
[31] Kim WY, Safran M, Buckley MR, et al. Failure to prolyl hydroxylate hypoxia-inducible factor alpha phenocopies VHL inactivation in vivo. EMBO J. 2006;25(19):4650–62.
[32] Xue X, Ramakrishnan S, Anderson E, et al. Endothelial pas domain protein 1 activates the inflammatory response in the intestinal epithelium to promote colitis in mice. Gastroenterology 2013;145(4):831–41.
[33] Li T, Yu B, Liu Z, et al. Homocysteine directly interacts and activates the angiotensin II type I receptor to aggravate vascular injury. Nat Commun 2018;9(1):11.
[34] Jin L, Lin X, Yang L, et al. AK098656, a novel vascular smooth muscle cell-dominant long noncoding RNA, promotes hypertension. Hypertension (Dallas, Tex : 1979) 2018;71(2):262–72.
[35] Fu Y, Gao C, Liang Y, et al. Shift of macrophage phenotype due to cartilage oligomeric matrix protein deficiency drives atherosclerotic calcification. Circ Res 2016;119(2):261–76.
[36] Gjurich BN, Taghavie-Moghadam PL, Galkina EV. Flow cytometric analysis of immune cells within murine aorta. Methods in molecular biology (Clifton, NJ) 2015;1339:161–75.
[37] Pan Y, Hui X, Hoo RLC, et al. Adipocyte-secreted exosomal microRNA-34a inhibits M2 macrophage polarization to promote obesity-induced adipose inflammation. J Clin Invest 2019;129(2):834–49.
[38] Shen M, Hu M, Fedak PWM, Oudit GY, Kassiri Z. Cell-Specific functions of ADAM17 regulate the progression of thoracic aortic aneurysm. Circ Res 2018;123(3):372–88.
[39] Duan C, Yang X, Zhang X, et al. Generation of monoclonal antibodies against MGA and comparison of their application in breast cancer detection by immunohistochemistry. Sci Rep 2015;5:13073.
[40] Sofi F, Marcucci R, Giusti B, et al. High levels of homocysteine, lipoprotein and plasminogen activator inhibitor-1 are present in patients with abdominal aortic aneurysm. Thromb Haemost 2005;94(5):1094–8.
[41] He L, Fu Y, Deng J, et al. Deficiency of fam3d (Family with sequence similarity 3, member D), a novel chemokine, attenuates neutrophil recruitment and ameliorates abdominal aortic aneurysm development. Arterioscler Thromb Vasc Biol 2018;38(7):1616–31.
[42] Sakalihasan N, Delvenne P, Nusgens BV, Limet R, Lapiere CM. Activated forms of MMP2 and MMP9 in abdominal aortic aneurysms. J. Vasc. Surg. 1996;24(1):127–33.
[43] Xie G, Liu Y, Yao Q, et al. Hypoxia-induced angiotensin II by the lactate-chymase-dependent mechanism mediates radioresistance of hypoxic tumor cells. Sci Rep 2017;7:42396.
[44] Krawczyk CM, Holowka T, Sun J, et al. Toll-like receptor-induced changes in glycolytic metabolism regulate dendritic cell activation. Blood 2010;115(23):4742–9.
[45] O'Neill LA, Hardie DG. Metabolism of inflammation limited by AMPK and pseudo-starvation. Nature 2013;493(7432):346–55.
[46] Tannahill GM, Curtis AM, Adamik J, et al. Succinate is an inflammatory signal that induces IL-1beta through HIF-1alpha. Nature 2013;496(7444):238–42.
[47] Lampropoulou V, Sergushichev A, Bambouskova M, et al. Itaconate links inhibition of succinate dehydrogenase with macrophage metabolic remodeling and regulation of inflammation. Cell Metab 2016;24(1):158–66.
[48] Laukka T, Mariani CJ, Ihantola T, et al. Fumarate and succinate regulate expression of hypoxia-inducible genes via TET enzymes. J Biol Chem 2016;291(8):4256–65.
[49] Liu PS, Wang H, Li X, et al. alpha-ketoglutarate orchestrates macrophage activation through metabolic and epigenetic reprogramming. Nat Immunol 2017;18(9):985–94.
[50] Xiao LJ, Lin P, Lin F, et al. ADAM17 targets MMP-2 and MMP-9 via EGFR-MEK-ERK pathway activation to promote prostate cancer cell invasion. Int J Oncol 2012;40(5):1714–24.
[51] Yevshin I, Sharipov R, Kolmykov S, Kondrakhin Y, Kolpakov F. GTRD: a database on gene transcription regulation-2019 update. Nucleic Acids Res 2019;47(D1):D100–D1d5.
[52] Wang L, Wang X, Kong W. [Recent advances of novel metalloproteinase ADAMTS family]. Sheng Li Ke Xue Jin Zhan 2008;39(1):49–52.
[53] Blaydon DC, Biancheri P, Di WL, et al. Inflammatory skin and bowel disease linked to ADAM17 deletion. N Engl J Med 2011;365(16):1502–8.
[54] Lee K, Zhang H, Qian DZ, Rey S, Liu JO, Semenza GL. Acriflavine inhibits HIF-1 dimerization, tumor growth, and vascularization. Proc Natl Acad Sci USA 2009;106(42):17910–15.
[55] del Porto F, Proietta M, Tritapepe L, et al. Inflammation and immune response in acute aortic dissection. Ann Med 2010;42(8):622–9.
[56] Son BK, Sawaki D, Tomida S, et al. Granulocyte macrophage colony-stimulating factor is required for aortic dissection/intramural haematoma. Nat Commun 2015;6:6994.
[57] Pearce EL, Pearce EJ. Metabolic pathways in immune cell activation and quiescence. Immunity 2013;38(4):633–43.
[58] O'Neill LA, Kishton RJ, Rathmell J. A guide to immunometabolism for immunologists. Nat Rev Immunol 2016;16(9):553–65.
[59] Wang T, Liu H, Lian G, Zhang SY, Wang X, Jiang C. HIF1alpha-Induced glycolysis metabolism is essential to the activation of inflammatory macrophages. Mediators Inflamm 2017;2017:9029327.
[60] Van den Bossche J, O'Neill LA, Menon D. Macrophage immunometabolism: where are we (Going)? Trends Immunol 2017;38(6):395–406.
[61] Isaacs JS, Jung YJ, Mole DR, et al. HIF overexpression correlates with biallelic loss of fumarate hydratase in renal cancer: novel role of fumarate in regulation of HIF stability. Cancer Cell 2005;8(2):143–53.
[62] Rizas KD, Ippagunta N, Tilson MD 3rd. Immune cells and molecular mediators in the pathogenesis of the abdominal aortic aneurysm. Cardiol Rev 2009;17(5):201–10.
[63] Jing SW, Wang YD, Kuroda M, et al. HIF-1alpha contributes to hypoxia-induced invasion and metastasis of esophageal carcinoma via inhibiting E-cadherin and promoting MMP-2 expression. Acta Med Okayama 2012;66(5):399–407.
[64] Ahn GO, Brown JM. Matrix metalloproteinase-9 is required for tumor vasculogenesis but not for angiogenesis: role of bone marrow-derived myelomonocytic cells. Cancer Cell 2008;13(3):193–205.
[65] Sari Y, Sanada H, Minematsu T, et al. Vibration inhibits deterioration in rat deep-tissue injury through HIF1-MMP axis. Wound Repair Regen 2015;23(3):386–93.
[66] Xu J, Sriramula S, Xia H, et al. Clinical relevance and role of neuronal AT1 receptors in ADAM17-Mediated ACE2 shedding in neurogenic hypertension. Circ Res 2017;121(1):43–55.
[67] Jiang C, Kim JH, Li F, et al. Hypoxia-inducible factor 1alpha regulates a SOCS3-STAT3-adiponectin signal transduction pathway in adipocytes. J Biol Chem 2013;288(6):3844–57.
[68] Cheloni G, Tanturli M, Tusa I, et al. Targeting chronic myeloid leukemia stem cells with the hypoxia-inducible factor inhibitor acriflavine. Blood 2017;130(5):655–65.